PHYSICAL REVIEW B VOLUME 25, NUMBER 12 15 JUNE 1982

Point-defect diffusion in a strained crystal

C. N. Tomé,* H. A. Cecatto,* and E. J. Savino
Departamento de Materiales, Comisión Nacional de Energía Atómica, Buenos Aires, Argentina
(Received 15 June 1981)

The diffusion equations for interstitials and vacancies in the field of an edge dislocation are numerically solved within a theoretical model that takes into account the full lattice and defect symmetry in the migration jump. The defect concentration is calculated within two different approximations: In one, only the defect drift contribution to the diffusion is considered, while in the other, the drift and gradient terms are included as well as a constant defect generation rate. In this second approximation the steady-state concentration is calculated. The influence on the solutions of an external uniaxial stress with different orientations with respect to the dislocation is studied. Numerical results for the dislocation sink strength are obtained for vacancies and interstitials in Cu. These are compared with previous approximations in the literature. The relevance of the results to the establishing of a radiation creep mechanism is discussed.

I. INTRODUCTION

When deducing a lattice defect diffusion equation the lattice symmetry is generally included both in the defect occupation and in the jump probability. However, to our knowledge, the detailed solution of complex problems that involve the diffusion in a space-varying strain field, for example, in a dislocation field, has been tackled only within a continuum model that involves a series expansion of those equations (i.e., Ham,[1] Margvelashvili and Saralidze,[2] Wolfer and Ashkin,[3] Rauch and Simon[4]). Some of the lattice influence on the process can be smeared out, and physically relevant effects may be lost in that expansion. The continuum approximation must be revised when diffusion in a strained crystal is studied. This revision was performed among others by Girifalco and Welch,[5] Kronmüller *et al.*,[6] Savino,[7] and Dederichs and Schroeder[8] (hereafter called DS). However, the first two sets of authors deduced diffusion equations which also lack some defect symmetry contributions that might be relevant to the process under study. Within a simple thermodynamic approximation, DS have obtained essentially complete expressions for the defect drift towards a sink in a strained crystal. The model deduced by them will be called "discrete approximation" to differentiate it from the continuum approximation previously mentioned.

Mathematical expressions for that discrete approximation, however, are cumbersome to evaluate when the defect-sink interaction field is complex, as in the previously mentioned case of drift towards a dislocation sink. The purpose of this work is to solve this drift problem for self-defects in a fcc structure. The effect of an external stress is also included in order to relate the solution of the problem to the irradiation creep phenomenon. As the results of this work are relevant to the rate theory of a medium under irradiation (Brailsford *et al.*[9]), the dislocation sink strengths are evaluated.

The plan of this paper is as follows: In Sec. II, based on the works of Savino[7] and DS,[8] we summarize the main facts about anisotropic diffusion in a strained lattice. In Sec. III the models adopted for calculating the point-defect–dislocation interaction energy are described. In Sec. IV the drift of point defects towards an edge dislocation is calculated within the discrete approximation by using an integration procedure inspired by that of Cottrell and Bilby[10] (CB) for the continuum model. This calculation highlights the differences between the results obtained with the discrete and with the continuum approximation, especially with respect to the effect of an external field. In Sec. V, the steady-state vacancy and interstitial concentration profiles around a dislocation in a medium irradiated at constant rate are calculated for a strained crystal. Those calculations allow the evaluation of the dislocation sink strengths for vacancies and interstitials and the influence of an external stress on those strengths. If the defect-strain field interaction energy is evaluated up to first order, the influence of an external stress on the sink strength is

zero within a pure continuum model, though the sink strength depends on that stress when higher-order terms are included on evaluating the interaction (Bullough and Willis[11]). In the calculations for the discrete approximation used here, only first-order terms are included for the interaction energy, and any effect of the external stress on the sink strength values arises precisely from that approximation to the problem.

II. DIFFUSION EQUATIONS IN THE DISCRETE AND CONTINUUM APPROXIMATION

Consider a lattice defect located at a given site i. In order to migrate from that site to a neighboring site j it must go through an activated state, most probably through the so-called saddle-point configuration n_{ij}. Kronmüller *et al.*[6] proposed the current density of defects at that point as a vector[12]

$$\vec{J}(\vec{R}_i)=\sum_{j\neq i}^{N}\sum_{n,n_{ij}}\frac{1}{2}[\nu_{ij}^{(n,n_{ij})}(\vec{R}_i)c^{(n)}(\vec{R}_i)-\nu_{ji}^{(n,n_{ij})}(\vec{R}_j)c^{(n)}(\vec{R}_j)]\vec{s}_{ij}\ , \tag{1}$$

where $c^{(n)}(\vec{R}_i)$ is the density of defects at i with orientation n; the total number of neighboring sites j that can be occupied by a single defect jump is N, and $\vec{s}_{ij}$ is a vector that joins the site i with the site j ($\vec{s}_{ij}=\vec{R}_j-\vec{R}_i$). The jump probability from i to j is taken as

$$\nu_{ij}^{(n,n_{ij})}(\vec{R}_i)=\nu_{0ij}^{(n)}\exp\{-[Q^{(n,n_{ij})}(\vec{R}_i)-E^{(n)}(\vec{R}_i)/kT\}\ , \tag{2}$$

where $Q^{(n,n_{ij})}(\vec{R}_i)$ is the lattice energy for a defect located at the saddle point in a n_{ij}-type jump which started in the $\vec{R}_i$ position (where the defect was originally located) with orientation n and with the corresponding lattice energy $E^{(n)}(\vec{R}_i)$. As discussed by DS on evaluating Eq. (2), one must consider that, depending on the defects symmetry and orientation n at $\vec{R}_i$, some jump paths (n_{ij}) or neighboring sites (j) are forbidden. In what follows the preexponential factor in Eq. (2) is taken as constant ($\nu_{0ij}^{(n)}=\nu_0$) and it is assumed that the equilibrium defect orientation at a given site is attained within a few jumps, i.e.,

$$c^{(n)}(\vec{R}_i)=c(\vec{R}_i)\frac{\exp[-E^{(n)}(\vec{R}_i)/kT]}{\sum_m \exp[-E^{(m)}(\vec{R}_i)/kT]}\ . \tag{3}$$

If defect concentrations and energies are considered to be values of a continuous and slowly varying function of the spatial coordinates, and $c^{(n)}(\vec{R}_j)\simeq c^{(n)}(\vec{R}_i)+\vec{s}_{ij}\cdot\vec{\nabla}c^{(n)}(\vec{R}_i)$, $E^{(n)}(\vec{R}_i)\ll kT$, and $\vec{s}_{ij}\cdot\vec{\nabla}E^{(n)}(\vec{R}_i)\ll kT$, after replacing Eqs. (2) and (3) in Eq. (1), it can be expanded in Taylor series and then be written as

$$\vec{J}(\vec{R}_i)=-\sum_{j=1}^{N}\sum_{n=1}^{n_0}\sum_{n_{ij}=1}^{N_{ij}}\frac{\nu_0}{2n_0}\exp\{-[Q^{(n,n_{ij})}(\vec{R}_i)-\bar{E}(\vec{R}_i)]/kT\}\times\{\vec{s}_{ij}\cdot\vec{\nabla}c(\vec{R}_i)+[c(\vec{R}_i)/kT]\vec{s}_{ij}\cdot\vec{\nabla}\bar{E}(\vec{R}_i)\}\vec{s}_{ij} \tag{4}$$

where N is the number of neighbor sites within the defect single-jump distance, n_0 the number of equilbrium orientations, and N_{ij} the number of different symmetry defect jumps. The average energy at the equilibrium site is defined as

$$\bar{E}(\vec{R}_i)=\frac{1}{n_0}\sum_{n=1}^{n_0}E^{(n)}(\vec{R}_i)\ . \tag{5}$$

Equation (4) can be written in vector notation as

$$\vec{J}(\vec{R})=-\underline{D}(\vec{R})\left[\vec{\nabla}c(\vec{R})+\frac{c(\vec{R})}{kT}\vec{\nabla}\bar{E}(\vec{R})\right]\ , \tag{6}$$

by defining a diffusivity tensor

$$D_{km}(\vec{R})=\sum_{j=1}^{N}\sum_{n=1}^{n_0}\sum_{n_{ij}=1}^{N_{ij}}\frac{\nu_0}{2n_0}\exp\{-[Q^{(n,n_{ij})}(\vec{R})-\bar{E}(\vec{R})]/kT\}s_{ij}^k s_{ij}^m \ . \tag{7}$$

Equation (7) reduces to the standard diffusivity constant for a stress-free lattice. However, $Q^{(n,n_{ij})}(\vec{R})$ in Eq. (7) cannot be generally expanded around a value $Q(\vec{R})$ due to its dependence on the saddle-point configuration via n_{ij} and n, and therefore, its intrinsic discontinuity at $\vec{R}$ (see DS).

III. DEFECT CONFIGURATION AND INTERACTION ENERGY

We shall consider the drift of a vacancy and a (100)-split dumbbell interstitial towards an edge dislocation in a fcc crystal. The point-defect equilibrium and saddle-point configurations are extensively discussed in the literature. Numerical values for Cu are taken from Schober's work,[13] where the dipole tensors for the equilibrium and saddle-point configuration are calculated by computer simulation. Schober has used different potentials for the atomic interaction. For our calculations the use of dipole tensor values based on different interatomic potentials gives some confidence that the dependence of the results on the lattice symmetry can be elucidated. According to the potential used by Schober for obtaining the dipole tensor this will be called either M (Morse), MM (modified Morse) or BM (Born-Mayer) dipole tensor.

Tomé and Savino[14] have shown that generally the main contribution to the anisotropy in the defect-dislocation interaction field comes from the anisotropic defect dipole tensor but not from the anisotropy of the elastic dislocation field, which is then taken as isotropic hereafter (Nabarro[15]). The interaction energy between a point defect and a dislocation in the presence of a strain field, when only the first-order (size) interaction is included, can be written as (Savino[7])

$$E_{\rm int}(\vec{R})=-\underline{p}^{pd}\times(\underline{e}^{\rm dis}(\vec{R})+\underline{\epsilon}^{\rm ext}(\vec{R}))\ . \tag{8}$$

In Eq. (8), $\underline{p}^{pd}$ is the dipole tensor for the point defect either at an equilibrium site or at the saddle-point location, while $\underline{e}^{\rm dis}$ and $\underline{\epsilon}^{\rm ext}$ stand for the dislocation and external strain fields, respectively.

IV. POINT-DEFECT DRIFT TOWARDS AN EDGE DISLOCATION

A. Theory

The number of point defects satisfies the conservation law (Fick's second law)

$$\frac{\partial c}{\partial t}=-\vec{\nabla}\cdot\vec{J} \tag{9}$$

which results from Eq. (6) in a second-order partial differential equation for c. If we are only interested in the drift contribution to the diffusion, the random-walk terms must be neglected in Eq. (9), and it reduces to a first-order differential equation in the space coordinates. This is possible whenever the term with ∇c in Eqs. (4) or (6) is negligible compared to the drift term $(c/kT)\nabla\bar{E}$. It can be seen that neglecting this term in these equations is equivalent to taking the concentration $c^{(n)}(\vec{R}_j)$ in Eq. (1) for $\vec{J}$ as constant in the neighborhood of $\vec{R}_i$. Within this approximation, the defect flow vector $\vec{J}$ is linear in concentration, i.e.,

$$\vec{J}=c\vec{v}\ , \tag{10}$$

an Eq. (9) reduces to

$$\frac{\partial c}{\partial t}+\vec{v}\cdot\vec{\nabla}c=\frac{dc}{dt}=0\ , \tag{11}$$

where the condition of defect conservation in a given volume element is implied (then $\vec{\nabla}\cdot\vec{v}=0$). Also, if $\vec{v}$ is irrotational ($\vec{\nabla}\times\vec{v}=0$), a potential function can be defined by

$$\vec{v}=-\vec{\nabla}\phi\ , \tag{12}$$

and with the above consideration on defect conservation ϕ is harmonic (i.e., $\vec{\nabla}^2\phi=0$). Also, a flow-line function ψ can be defined by

$$\vec{v}\cdot\vec{\nabla}\psi=0\ . \tag{13}$$

The functions $\phi=$const and $\psi=$const define the characteristic coordinates of the problem. If the initial condition for the concentration is

$$c(\vec{r},t=0)=c^*(\vec{r})\ , \tag{14}$$

the solution of (11) is

$$c(\vec{r},t)=c^*\left[\vec{r}-\int_0^t(\vec{v}\hat{\psi})\hat{\psi}\,dt\right], \tag{15}$$

where $\hat{\psi}$ is an unit vector tangent to the characteristic line ψ defined by Eq. (13) at $\vec{r}$. Equation (15) shows that solving Eq. (11) is equivalent to obtaining the characteristic functions ϕ and ψ for every point in space.

If the diffusivity and the defect dipole tensors are isotropic and space independnt, i.e.,

$$D_{km}=D\delta_{km} , \tag{16}$$

$$p_{ij}^{pd}=p\delta_{ij} , \tag{17}$$

then Eq. (8) reduces in an isotropic continuum to

$$E_{\text{int}}(\vec{r})=A\frac{\sin\theta}{r}-p\,\text{tr}\underline{\epsilon}^{\text{ext}} , \tag{18}$$

where $A=pGb/2\pi(1-\nu)$, with $\vec{b}$ the dislocation Burgers vector, G the Young's modulus, ν the Poisson's ratio, and the polar coordinates r,θ,z, with z along the dislocation line and r measured from this line. Equation (11) was solved by Cottrell and Bilby (CB) under the assumptions of Eqs. (16)–(18) and considering the dislocation core as an ideal sink, i.e., with boundary conditions

$$c(r=0,t)=0 , \tag{19}$$

and with initial conditions

$$c(\vec{r},t=0)=c_0H(r) . \tag{20}$$

Here, $H(r)$ is the Heaviside function and r is the modulus of the vector $\vec{r}$. CB's solution of Eq. (11) results with a time t in a zone depleted of defects which have been absorbed at the sink, and this zone is bounded by the line

$$R^{\text{CB}}(\theta,t)=\left[\frac{2ADt}{kT}\right]^{1/3}\cos\theta \times\left[\frac{\pi}{2}-\theta-\frac{\sin2\theta}{2}\right]^{-1/3} . \tag{21}$$

Outside this zone the concentration is c_0. R^{CB} in Eq. (21) is the locus of points $\vec{r}$ on a characteristic line $\psi_s=$const that satisfies the relation

$$t=\int_{\vec{r}}^{0}\left[\frac{\partial\psi_s}{\partial t}\right]^{-1}d\psi_s . \tag{22}$$

As previously discussed, the influence of the lattice symmetry is retained when the flux vector $\vec{J}(c,r,\theta)$ is defined either by Eq. (1) or Eq. (6). Equation (9) can be reduced to Eq. (11) by neglecting in the evaluation of $\vec{J}$ terms which contain spatial derivatives of c or, equivalently, assuming $c(\vec{R}_j)=c(\vec{R}_i)=c_0$ in Eq. (1); in this case, Eq. (10) is a valid approximation. The flow lines ψ can be obtained afterward either analytically or simply by numerical or graphical methods. For a conservative and irrotational defect flux, if the boundary conditions of Eqs. (19) and (20) are adopted, the solution of Eq. (11) is

$$c(\vec{r},t)=c_0H(r-R(\theta,t)) \tag{23}$$

where $\vec{r}=r(\cos\theta,\sin\theta)$ and $R(\theta,t)$ is the absolute value of the vector

$$\vec{R}=\int_0^t(\vec{v}\cdot\hat{\psi})\hat{\psi}\,dt$$

collinear with $\vec{r}$. Equation (22) can be used for obtaining the boundary between the depleted and constant density (c_0) zones for a given time t.

We have adopted a step-by-step numerical interpolation method for constructing the flow lines $\psi=$const. This is based on evaluating the flow vector $\vec{J}$ tangent to that line. In the discrete approximation, $\vec{J}$ is given by Eq. (1) with $c(\vec{R})=c_0$ and by assuming an edge-dislocation interaction with point defects of different symmetry via their dipole tensor values, while the dislocation field is taken as the continuum field at the defect position. This numerical procedure to solve Eq. (22) enables us to map the depleted zone contour $R(\theta,t)$ for a given defect symmetry, that is a given $\vec{J}$ form. Evidently this method can also be used to solve Eq. (11) when the flow vector $\vec{J}$ is calculated under the same approximations as those made by CB. The comparison between the numerical solution and the analytic one of Eq. (21) is used as a test for the accuracy of the numerical method.

B. Vacancy drift

The numerical method previously described is applied to solve Eq. (11) for the vacancy and interstitial drift towards an edge dislocation along a $\{111\}$ plane with a $\langle 110\rangle$ Burgers vector. Although the omission of the diffusion term in Eq. (9) implies that the solution is only valid for unrealistically short times, a comparison with the equivalent one obtained within a continuum model by CB will provide some insight about the relevance of including (via the discrete approximation) the lattice and defect symmetry into $\vec{J}$. In this section, the M point-defect dipole tensor values are used.

Results for the vacancy drift towards the dislocation in the absence of an external stress are shown in Fig. 1. There, the depleted zone boundary $R(\theta,t)$ is drawn as a function of the reduced

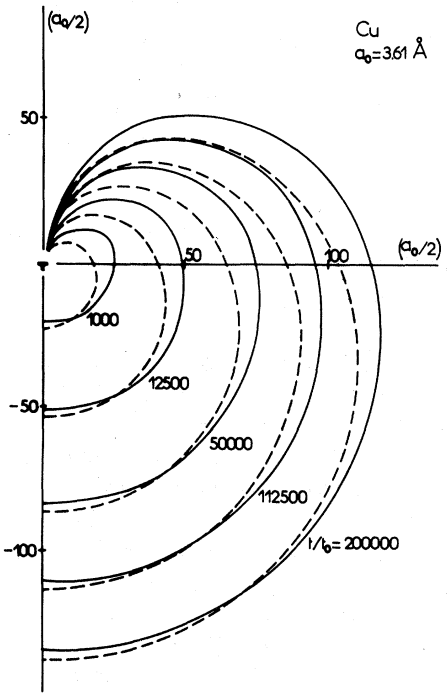

FIG. 1. Vacancy-depleted zone around an edge dislocation in Cu at 300 K. The time is taken in units of $t_0=\nu_0^{-1}\exp(Q_0/kT)$, and M dipole tensors (Ref. 13) are used. Solid line: "discrete approximation," Eq. (1). Dashed line: $R^{CB}(\theta,t)$ and "discrete approximation" with zero dipole tensor at the saddle point.

time

$$t_0=\frac{1}{\nu_0}\exp\left[\frac{Q_0}{kT}\right], \tag{24}$$

where Q_0 is the migration energy in a stress-free lattice. A plane perpendicular to the dislocation line and that contains the Burgers vector is considered. Solid lines correspond to a flux vector $\vec{J}$ evaluated with Eq. (1). The equilibrium dipole tensor for the vacancy is spherically symmetric as in Eq. (17), while the corresponding dipole tensor in the saddle-point configuration is anisotropic (Schober[13]). If the interaction between the dislocation and the defect at the saddle point is neglected in $\vec{J}$, Eq. (1), the numerical solution should converge to the corresponding analytic solution of CB provided the proper values of A are adopted in Eq. (18). This is indeed the case and it is found (see Fig. 1) that the numerical solution obtained agrees closely with the analytic solution (21). By comparing this analytic solution [the dashed line for $R(\theta,t)$ in Fig. 1] with the numerical solution in the discrete approximation that includes the full lattice effects (the solid line in Fig. 1), significant differences are found. These differences are then mainly due to the inclusion of the vacancy-dislocation interaction at the saddle-point configuration in the diffusion equation.

C. Vacancy and interstitial drift to a dislocation in an externally strained crystal

From Eqs. (6) and (7) it can be seen that when the full lattice and defect anisotropy are included in evaluating a defect flow vector $\vec{J}$ in a complex strain field, it may affect the defect drift via local changes in the anisotropy of the diffusivity tensor. For studying this effect we shall assume that, in addition to the dislocation field, a homogeneous strain field corresponding to uniaxial stress is applied to the crystal,

$$\epsilon_{xx}^{ext}=\epsilon,\quad \epsilon_{yy}^{ext}=\epsilon_{zz}^{ext}=-\nu\epsilon\ . \tag{25}$$

Two different orientations of this field with respect to the dislocation are studied: The x direction (I) parallel to the [110] Burgers vector and (II) perpendicular to it and to the dislocation line. For the sake of numerical accuracy and in order to enhance the effect, a relatively large field of $\epsilon=10^{-2}$ was used for the numerical calculations in the discrete approximation. The flux lines and depleted zone boundaries for the vacancy migration are plotted in Figs. 2(a) and 2(b), respectively. Figure 2(b), when compared to Fig. 1, shows that there is a net change in shape and magnitude of the depleted zones as a function of the orientation of the external field.

In Fig. 3, the depleted zones and flow lines for the interstitial drift are plotted. For the case of the interstitial drift, there are several effects included in the calculation that makes it diverge from the CB analytic solution for point-defect diffusion in a dislocation field. These effects are as follows: (i) the defect equilibrium and saddle-point symmetries are included in the diffusivity constant, which has a tensorial character, (ii) the corresponding defect dipole tensors are both anisotropic, (iii) the thermal equilibrium distribution of interstitial orientations (3) is assumed at a given site, and (iv) for a given orientation of the interstitial at a site only eight nearest-neighbor sites can be reached via a single jump (see DS).

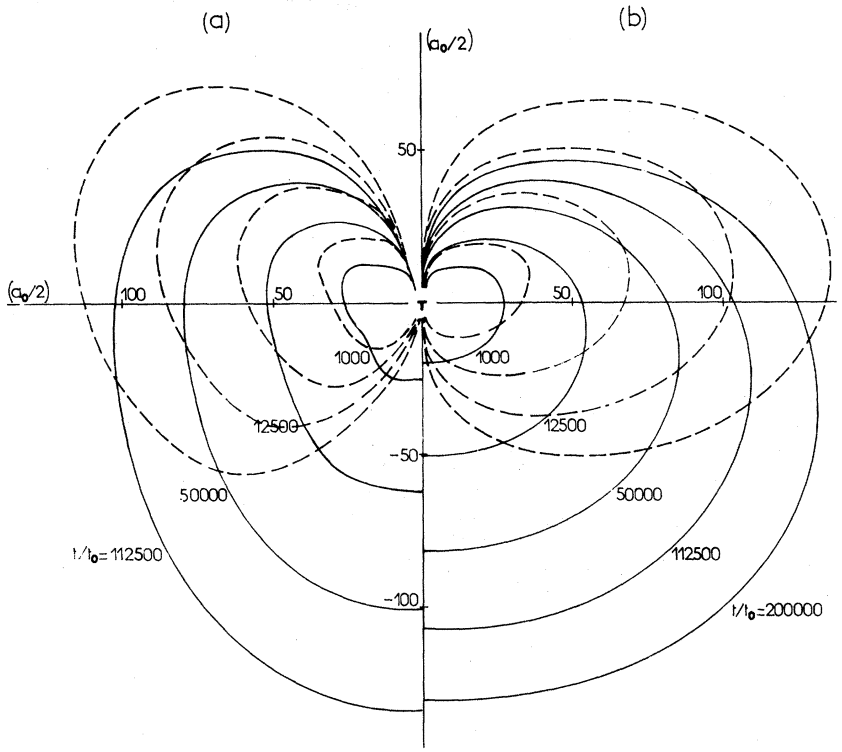

FIG. 2. Same as Fig. 1 but with an external uniaxial stress field with strain $\epsilon=\sigma_x/E=0.01$. Solid line: flow front (depleted zone boundary). Dashed line: flow line. (a) Orientation I with the x direction parallel to $\vec{b}$ and perpendicular to the dislocation line vector $\vec{\xi}$. (b) Orientation II with the x direction perpendicular to $\vec{b}$ and to $\vec{\xi}$.

V. STEADY-STATE SOLUTION AND SINK STRENGTH CALCULATION

A. Hollow cylinder sink strength

When studying different problems such as aging, recovery, radiation damage, etc., it is valuable to determine the dislocation's defect capture efficiency or what is commonly defined as capture radius or, equivalently, the sink strength. Any of these parameters allows replacement of the real medium with a discrete distribution of dislocations by an effective or lossy medium where the defect sinks are smeared out and their capture efficiency is adequately weighted. The whole concept of lossy medium is reviewed by Brailsford and Bullough[16] in a recent paper to which we refer the reader.

In a medium under irradiation there is a time-dependent production of defects. If the production rate is assumed to be constant (K), Eq. (9) transforms into

$$\frac{\partial c}{\partial t}=-\vec{\nabla}\cdot\vec{J}+K\ , \tag{26}$$

where $\vec{J}$ is now the defect flow towards any sink in the crystal and c is the interstitial or vacancy concentration. If there is more than one sink in the medium, but all are of the same type, say, dislocations, Eq. (26) can be replaced by the effective medium equation.

$$\frac{\partial\langle c\rangle}{\partial t}=Dk_D^2\langle c\rangle+K\ . \tag{27}$$

Here, $\langle c\rangle$ is the space-averaged concentration value, D the isotropic diffusivity, as in Eq. (7) for a stress-free crystal, and k_D^2 is the dislocation sink strength. In several problems of technological interest, steady state may be assumed, i.e., $\partial c/\partial t=0$ (see, however, Rauch and Simon[4]). Equation (27) provides then a way of calculating k_D^2 as

$$k_D^2=\frac{K}{D\langle c\rangle}\ . \tag{28}$$

For a periodic or random array of dislocations, Eq. (26) is consistently solved for the steady state, and the calculated concentration is averaged over an appropriate volume. If a periodic array of dislocations is assumed, each dislocation must be along the center axis of a cylinder of radius

$$R^{\text{ext}}=(\pi\rho_D)^{-1/2}\ , \tag{29}$$

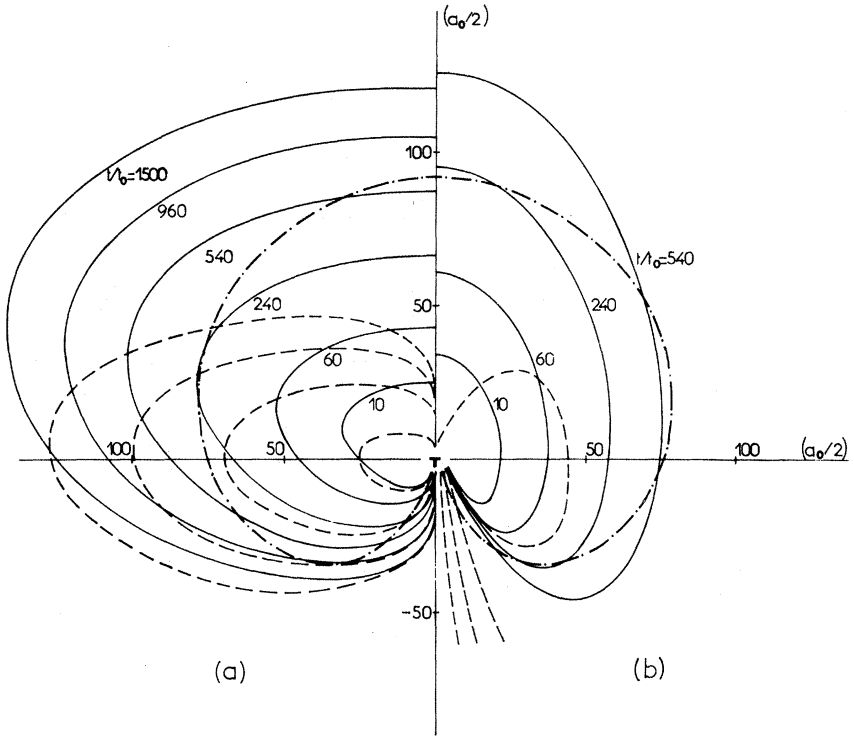

FIG. 3. Same as Fig. 2 but for the dumbbell interstitial and $\epsilon=0.01$. Dash-dot line (—·—·—·) is the flow front (depleted zone boundary) for the interstitial under a zero external field and $t/t_0=540$.

where ρ_D is the dislocation density. Periodicity imposes the condition

$$\vec{J}(R^{\text{ext}})=0 \ . \tag{30a}$$

An extreme simplification of the problem is obtained by neglecting the defect-dislocation elastic interaction of Eq. (8). Then the dislocation is simulated as a hollow cylinder of radius r_c centered at the dislocation line where

$$c(r)=0 \ \text{ if } r\leq r_c \ . \tag{30b}$$

The sink strength so obtained is

$$k_D^2=2\pi\rho_D\frac{(1-\alpha^2)}{(-\ln\alpha-\frac{3}{4}+\alpha^2-\frac{1}{4}\alpha^4)} \ , \tag{31}$$

where $\alpha=r_c/R^{\text{ext}}$.

Some authors replace the boundary condition of zero flux at R^{ext} by the condition

$$c(R^{\text{ext}})=c_0 \ . \tag{32}$$

However, Eq. (32) will only be appropriate for a random distribution of dislocations, and c_0 should be related to the defect production rate and the geometry of the problem. If the sink strength of Eq. (28) is evaluated for the concentration obtained, assuming that the condition of Eq. (32) is valid, it yields

$$k_D^2=2\pi\rho_D\frac{1}{\left[-\ln\alpha-\frac{1}{2}+\frac{\alpha^2}{2}\right]} \ . \tag{33}$$

If the point-defect—dislocation interaction is included in Eq. (26), even at steady state the problem becomes much more difficult to solve, and no complete analytic solution seems to exist. Several authors (Burke and Nix,[17] Rauch and Simon,[4] Wolfer and Ashkin,[3] and Margvelashvili and Saralidze[2]) have solved the diffusion equation by choosing appropriate boundary conditions at $r=R^{\text{ext}}$. Brailsford *et al.*[9] also suggested simulating the drift term by a net flux increment near the dislocation core, and the same authors[16] recently proposed an approximate solution which includes the interaction field. However, this solution is valid only under certain conditions, e.g., it would be valid for interstitials in Cu only if they produced spherically symmetric distortion field.

B. Numerical solution

Given a flow vector $\vec{J}(\vec{r})$, Eq. (26) can be solved numerically for the steady state

$$\vec{\nabla}\cdot\vec{J}=K \tag{34}$$

within a finite difference scheme. For the case of diffusion in a straight dislocation field, cylindrical coordinates (R,θ) and a mesh of nodal points are chosen as shown in Fig. 4. For this coordinate system

$$(\bar{R}_M,\bar{\theta}_N)=\left[\left[\frac{R_M^2+R_{M+1}^2}{2}\right]^{1/2},\left[\frac{\theta_N+\theta_{N+1}}{2}\right]\right]$$

is the position of the geometrical center of an element $(R_{M,M+1},\theta_{N,N+1})$, where M runs over the radial nodes and N over the angular ones; Eq. (34) is then written as

$$[J_r(R_{M+1},\bar{\theta}_N)R_{M+1}-J_r(R_M,\bar{\theta}_N)R_M](\theta_{N+1}-\theta_N)+[J_\theta(\bar{R}_M,\theta_N)-J_\theta(\bar{R}_M,\theta_{N+1})](R_{M+1}-R_M)$$
$$=K\left[\frac{\theta_{N+1}-\theta_N}{2}\right](R_{M+1}^2-R_M^2)\,, \tag{35}$$

where the flow vector is expressed in cylindrical coordinates $\vec{J}=J_r\hat{e}_r+J_\theta\hat{e}_\theta$. The flow vectors of Eq. (1), needed to evaluate Eq. (35) in the discrete approximation, can be expressed as a linear function of the concentrations $c(\bar{R}_M,\bar{\theta}_N)$. This is done by assuming an equilibrium defect lattice site located at the position where $\vec{J}$ is to be evaluated, that is, at the (R,θ) positions of Eq. (35), and linearly interpolating the concentration at this lattice site and at its neighbor sites [$c(R_i)$ and $c(R_j)$ in Eq. (1), respectively] from the concentrations $c(\bar{R}_M,\bar{\theta}_N)$ associated with the center of the six nearest elements. By the above procedure, Eq. (34) is reduced to a system of linear equations in the concentrations at the center of the elements. These concentrations with the appropriate boundary conditions can now be solved by matrix inversion.

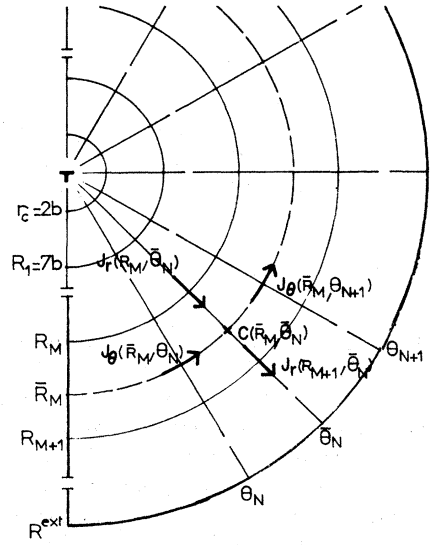

FIG. 4. Mesh of cylindrical coordinates and flow vectors used for numerically solving Eq. (34) by finite differences.

An appropriate nodal spacing must be chosen for ensuring convergency in a finite-difference method. We have divided a circle centered at the dislocation by an integer number of angular nodes separated by an angle $\Delta\theta$ and applied the recursive formula

$$R_{M+1}=(1+\Delta\theta)R_M \tag{36}$$

for the radial nodes. For all the calculations the conditions of Eq. (30) are adopted where R^{ext} is taken as a radial node and ρ_D is determined by using Eq. (29). The first radial node is always taken at $R_1=7b$ and the boundary condition of Eq. (30b) is imposed at $r_c=2b$.

The solution for the concentration must satisfy the linear system of equations, and the total number of defects must be conserved, that is,

$$K\pi(R^{ext2}-R_1^2)=\sum_N J_r(R_1,\bar{\theta}_N)R_1\Delta\theta\,, \tag{37}$$

where N runs over all the angular increments $\Delta\theta$, for $\theta=0,2\pi$. The average concentration necessary for evaluating k_D^2 in Eq. (28) is calculated by

$$\langle c\rangle=\frac{\sum_{M=1}^{M_T}(R_{M+1}^2-R_M^2)\sum_{N=1}^{N_T}c(\bar{R}_M,\bar{\theta}_N)}{N_T\sum_{M=1}^{M_T}(R_{M+1}^2-R_M^2)}\,, \tag{38}$$

where the sum runs over the geometrical centers $(\bar{R}_M,\bar{\theta}_N)$ of the M_TN_T net elements located in the region betwen R_1 and R^{ext}.

C. Vacancy and interstitial concentration

By using the numerical method previously described, the steady-state vacancy and interstitial distribution around an edge dislocation with line and Burgers vector $\vec{\xi}\|[11\bar{2}]$ and $\vec{b}\|[1\bar{1}0]$ in a crystal either externally strained or unstrained was calculated in the discrete approximation of Eq. (1). Boundary conditions of Eq. (30) are adopted.

In Figs. 5(a) and 5(b), the concentration at 300 K of vacancies and interstitials around the dislocation in a crystal free of external stresses is sketched. In these calculations the MM dipole tensors are used for the point defects. The concentration distribution for the vacancy is nearly independent of the angle and resembles the one of the hollow cylinder. For the interstitial the steady-state concentration is enhanced on the tensile side of the dislocation near the core and, conversely, depleted at the compressive side. Also for both types of defects the concentration is nearly independent of the angle at $r \simeq R^{\text{ext}}$.

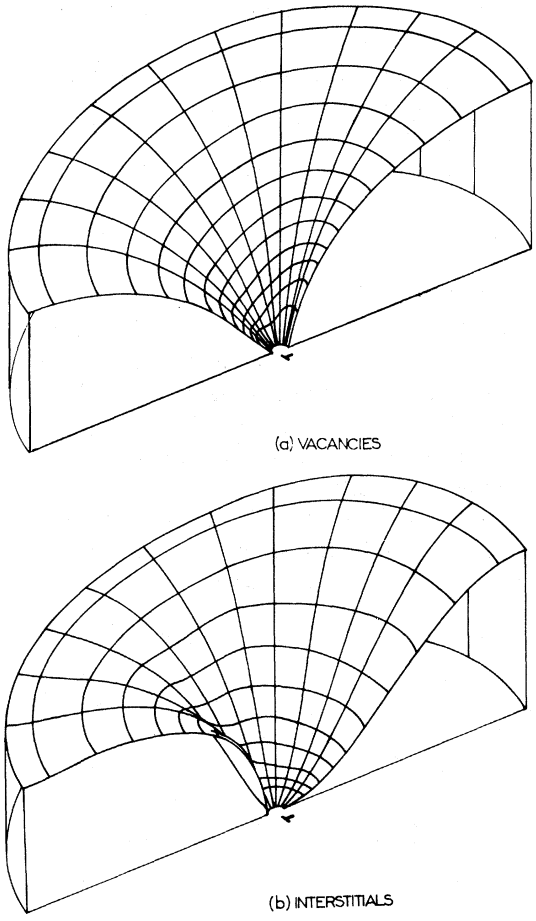

FIG. 5. (a) Vacancy concentration contour. (b) Interstitial concentration contour around the dislocation for the steady state and for $\epsilon^{\text{ext}}=0$ (arbitrary units). MM sets of dipole tensors (Ref. 13) is used, $T=300$ K.

D. Dislocation sink strength in a stress-free crystal

The steady-state defect distribution around the edge dislocation in a stress-free crystal, which was obtained by finite differences, is used, together with Eqs. (28) and (38) to calculated the sink strength. Some results for k_D^2/ρ_D are plotted in Fig. 6 as a function of the dislocation density. The MM dipole tensor is used for the point defects, and calculations for 300 and 900 K are reported. The discrete approximation results are compared with (i) the same approximation but taking the interaction at the vacancy saddle point as zero, and (ii) the hollow cylinder models with Eqs. (31) and (33) for different dislocation capture radii r_c. The figure shows that, for the same capture radius r_c, the numerical discrete approximation gives larger sink strength than any of the others. Within a hollow

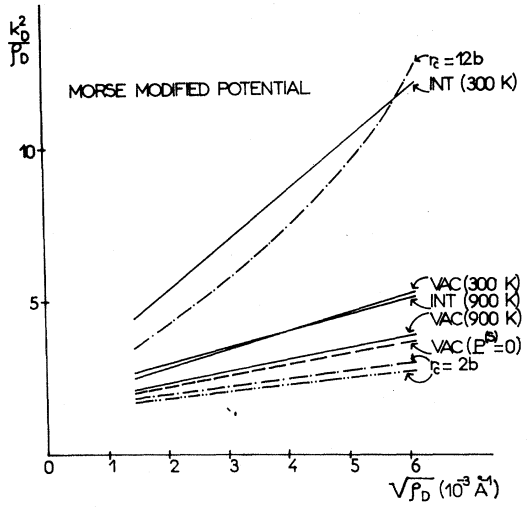

FIG. 6. Dislocation sink strengths in units of dislocation density, k_D^2/ρ_D, vs $\rho_D^{1/2}$. Solid line (——): MM set of dipole tensors (Ref. 13) are used for the vacancy and interstitial in Eq. (1) and for 300 and 900 K. Dashed line (— — —): vacancy case with a saddle point dipole tensor equal to zero; it gives temperature-independent results. Dash-dot line (—·—·—·): hollow cylinder sink strength with boundary conditions of Eq. (30) and r_c values as indicated. Dash-double-dot line —··—··—): hollow cylinder sink strength with the boundary condition $c(R^{\text{ext}})=c_0$.

cylinder approximation and boundary conditions of Eq. (30) or (32) a relatively large capture radius of $r_c=7b$ and $r_c=5.5b$, respectively, must be adopted for obtaining agreement between the k_D^2 calculated with this model and with the discrete one for the vacancy case.

The fact that, for this case, perfect agreement in the curve shape dependence is obtained proves that the sink strength is mainly determined by the diffusive and not by the drift term. Also, the discrete approximation is the only one that gives a temperature-dependent sink strength. This dependence arises from the inclusion of the saddle-point vacancy-dislocation interaction energy in Eq. (1). This can be seen by comparing the full discrete approximation with that in which the interaction at the saddle point was not included and which shows no temperature dependence. This result is in accordance with the theoretical prediction of DS in the sense that, for stationary conditions, the jump rate of point defects across the saddle-point energy barrier only depends on the height of the barrier and not on its relative height with respect to the valley. In Fig. 6 it is also seen that in the discrete approximation the dislocation bias for the interstitial is, as expected, much larger than for the vacancy. If at 300 K we want to fit the sink strength by an effective capture radius in the hollow cylinder approximation, a very large one must be chosen (that corresponding to $r_c=12b$ is shown in Fig. 6). Also, for interstitials at that temperature the dependence of the sink strength on the dislocation density cannot be approximated by a hollow cylinder model. These facts prove that including a relatively large drift term within the discrete approximation affects both the value of the sink strength and its parametric dependence on sink density.

E. Dislocation sink strength in a strained crystal

If a continuum approximation for the diffusion flow is used, Eq. (6), and lattice effects are not included in the diffusivity constant of Eq. (7), the dislocation sink strength for a paint defect is only affected by a uniaxial external strain when terms of order higher than the first considered in Eq. (8) are included in the interaction energy. We shall see that this is not the case in the discrete approximation. We shall always use the first-order equation (8) for the interaction energy of the defect with any strain field at the crystal. For the edge dislocation with $\vec{\xi}\|[11\bar{2}]$, $\vec{b}\|[1\bar{1}0]$ we shall consider the crystal to be strained as described by Eq. (25). Three different orientations of the x direction for the strain field are studied:

(I) parallel to the $[1\bar{1}0]$ Burgers vector,

(II) perpendicular to it and the dislocation line, and

(III) perpendicular to it and parallel to the dislocation line.

The sink strength dependence on the strain field orientation and magnitude is not simple. We plot in Fig. 7(a) the dislocation sink strength for the MM vacancy dipole tensor as a function of the uniaxial strain value for the three strain orientations previously described, taking the dislocation density as a parameter. Calculations for external strains ϵ in Eq. (25), varying between 0 and 5×10^{-3} are reported. It can be seen in Fig. 7(a) that for orientations II and III the sink strength increases as a function of the strain, with the strength for case III being always larger than that for case II regardless of the dislocation density.

For orientation I, where the axis for the uniaxial stress responsible for ϵ is parallel to the Burgers vector, the calculated sink strength remains approximately constant for small strain values (it

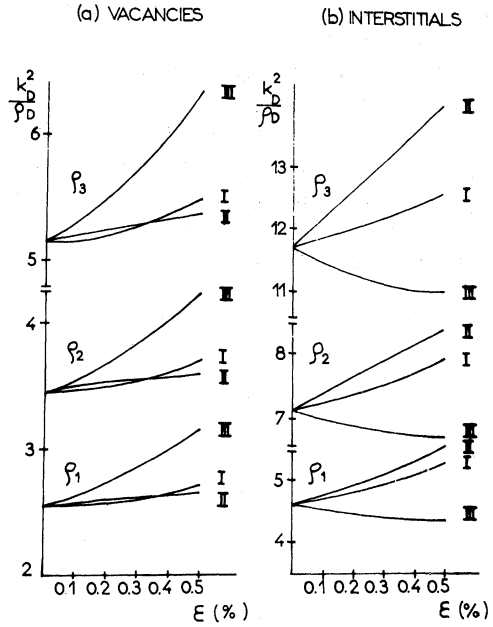

FIG. 7. Dislocation sink strength as a function of the external strain field ϵ, (a) for vacancies, (b) for interstitials. MM dipole tensors are used, $T=300$ K. Dislocation densities: $\rho_1=2.5\times10^{10}/\text{cm}^2$, $\rho_2=9.5\times10^{10}/\text{cm}^2$, $\rho_3=35.6\times10^{10}/\text{cm}^2$. Orientations I, II, and III as described in the text.

may even decrease somewhat) and then shows a large increase for larger strains, until finally the line for this orientation crosses the one corresponding to orientation II at strains between 3 and 4×10^{-3}. For the interstitial (simulated by MM dipole tensors), the dislocation sink strength is plotted in Fig. 7(b) as a function of the strain value. Here it is seen that for orientations I and II, there is a clear sink strength increase as a function of strain, while for orientation III there is a decrease. Also, the increment is larger for orientation II than I. This is contrary to what Savino[7] has assumed, based on a much simpler model and also contrary to the prediction of Bullough and Willis,[11] which considers second-order elasticity for the point-defect—dislocation interaction energy.

F. SIPA-AD creep

From the technological point of view, it is interesting to see if the stress-induced preferential attraction due to anisotropic diffusion (SIPA-AD) of the radiation produced defects may generate a net dislocation climb and a permanent strain rate (creep) under a constant applied uniaxial stress. This question is answered in the affirmative, and the creep effects are planned to be discussed in a forthcoming paper.[18]

In this paper we shall only advance that, as proposed by Bullough and Hayns[19] with a simplified model that only includes network dislocation as point-defect sinks and no recombination between interstitials and vacancies, the crystal strain rate in the external stress direction will depend on the sink strength for interstitials and vacancies as

$$\frac{1}{K}\frac{d\epsilon_{\rm I}}{dt}=K_i^2-K_v^2\,, \tag{39}$$

where

$$K_i^2=\frac{\frac{2}{3}k_{i_{\rm I}}^2-\frac{1}{3}(k_{i_{\rm II}}^2+k_{i_{\rm III}})}{k_{i_{\rm I}}^2+k_{i_{\rm II}}^2+k_{i_{\rm III}}^2}$$

and

$$K_v^2=\frac{\frac{2}{3}k_{v_{\rm I}}^2-\frac{1}{3}(k_{v_{\rm II}}^2+k_{v_{\rm III}}^2)}{k_{v_{\rm I}}^2+k_{v_{\rm II}}^2+k_{v_{\rm III}}^2}\,,$$

and $k_{i_L}^2$ and $k_{v_L}^2$ stand for the dislocation sink strengths for the interstitial and vacancy with the crystal strained in orientation L (L=I,II,III). Equation (39) is plotted in Fig. 8 as a function of the external strain value using the sink strength shown in Figs. 7(a) and 7(b) and also those corresponding to 900 K. It can be seen that a finite creep rate is predicted by the model proposed above.

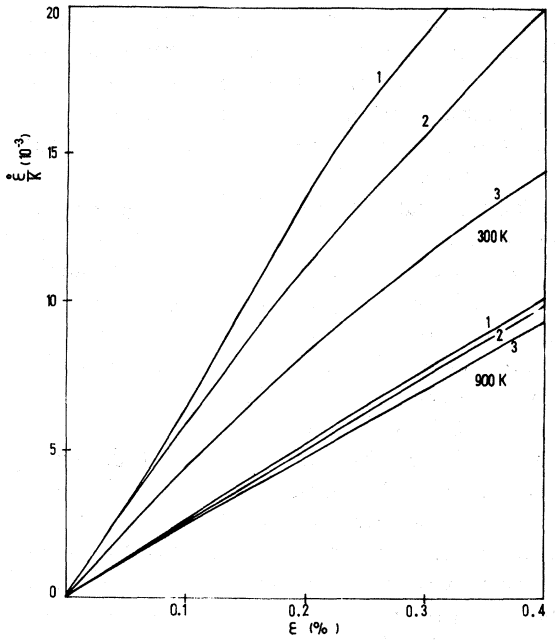

FIG. 8. Creep strain rate per unit defect production rate against external strain field $\epsilon=\sigma/E$ produced by an uniaxial stress σ in the x direction. The sink strengths of Fig. 7 plus the equivalent ones at 900 K are used for the calculations. 1, 2, and 3 stand for ρ_1, ρ_2, and ρ_3, respectively.

VI. SUMMARY AND CONCLUSIONS

We have studied in this paper the problem of vacancy and interstitial migration due to the drift produced by a dislocation elastic strain field. Our main aim has been to show the influence of including explicitly in the diffusion equation the full defect symmetry both at equilibrium and at the activated state. The diffusion model for point defects in a strain field proposed by Kronmüller *et al.*,[6] Savino,[7] and Dederichs and Schroeder[8] is used. This model and the expression for the interaction energy have been reviewed in Secs. II and III of this paper. Even for an isotropic spherically symmetric point defect, the inclusion of the interaction with a dislocation into the diffusion Eq. (26) makes that equation rather complex to be solved analytically. As discussed in the paper this equation has been solved for the steady state by

neglecting the diffusion term (Cottrell and Bilby[10]), or with a Bessel series expansion (Ham[1] and Rauch and Simon[4]). If the full point-defect symmetry at the equilibrium and saddle-point configurations is considered, an anisotropic diffusivity tensor (7) results for the diffusion equation and the problem of migration in a dislocation field must be solved numerically. We have solved in Sec. III the problem of vacancies and interstitial diffusion in an externally strained crystal within the discrete approximation for the diffusion of point defects in a dislocation field and using a pure drift approximation equivalent to the one used by CB within the continuum approach. There, the flow lines and flow fronts for the zone depleted of defects are compared for both kinds of defects and different orientations of an externally applied uniaxial stress field. It is evident from Eq. (6) that in the continuum approximation of CB,[10] Ham,[1] etc., the diffusion equation is not affected by the orientation of the external field unless terms of order higher than the linear ones are considered in the interaction field (Wolfer and Ashkin[3] and Bullough and Willis[11]). The local anisotropy in the diffusivity tensor is the main effect that the "discrete approach" introduces for the diffusion of vacancies and interstitials in a strain field. This means that the defect flow changes for different orientations of the external field via a coupling between this field, which affects the anisotropy of the diffusivity, and the gradient of the dislocation interaction field. The strain orientation influence can be clearly seen in Figs. 1–3 by comparing the cases with and without external strain fields. When the vacancy field is spherically symmetric in equilibrium, the external strain field only affects the dislocation drift via the interaction energy at the saddle-point configuration. The (100) dumbbell interstial in a fcc crystal is not only anisopic in equilibrium, but it can take three different orientations with different interaction energy with a strain field. We have assumed that, on the average, equilibrium with regard to orientations is attained instantaneously, and Eq. (3) was adopted throughout the work. In this case, Eq. (6) is valid for any defect symmetry.

The drift contribution considered in Sec. IV may only dominate the diffusion at very short times. In order to calculate the dislocation strength for interstitials and vacancies we have therefore solved Eq. (34) for diffusion at steady state in a dislocation field including the concentration gradient, the defect–strain-field interaction, a defect production term, an external strain field, and appropriate boundary conditions. The influence of the drift term, as included in the model, on the dislocation sink strength is clearly shown in Fig. 6, where the numerical results are compared against the hollow cylinder approximation, which only considers the dislocation as a cylindrical, perfect sink, but neglects any interaction field. We found that for a weak interaction field (vacancy), or a large interaction field (interstitial), but at high temperatures ($T \gtrsim 900$ K), the hollow cylinder approximation sink strength approximately agrees with the numerical calculation if an appropriate capture radius is chosen. The effect of the interaction field is only to increase the effective capture radius. This is not the case for a large interaction field (interstitial at 300 K in Fig. 6); although a big capture radius that approximates the numerical result for a given dislocation density can be chosen, the strength dependence on sink concentration cannot be fitted satisfactorily by the hollow cylinder model.

In Sec. V, a crystal containing a periodic distribution of equivalent edge dislocations is taken and uniaxially stressed in three different directions: (I) parallel to the dislocation Burgers vector, (II) perpendicular to it and the dislocation line, and (III) perpendicular to the Burgers vector and parallel to the line. The calculated sink strengths are strongly dependent on the external strain. It is interesting to see in Fig. 7 that a large effect of the strain appears in orientation III, and the strength k^2_{III} increases for the vacancies and decreases for the interstitials. This can be easily understood by looking at the symmetry of the saddle-point configuration for either defect and remembering than for the strain orientation III the crystal is strained in tension in the dislocation line direction, while in perpendicular directions it is uniformly compressed. Then the vacancy diffusivity on the perpendicular plane is always increased by this external field, so $\langle c_v \rangle$ is decreased, and the interstitial diffusivity is decreased, so $\langle c_i \rangle$ is increased. For orientations I and II, the analysis is not so simple but significant effects seem to take place mainly for interstitial.

Finally, the calculated sink strengths in the presence of an uniaxial homogeneous stress field are used to evaluate the creep rate in a lossy medium with a single sink type: a homogeneous distribution of edge dislocations. It is seen in Fig. 8 that for this very simplified model, which does not include either recombination or other sinks, sensible values (i.e., larger than the experimental ones) for

the irradiation creep are obtained. This subject is planned to be discussed in a forthcoming paper.[18] Here, we want only to stress that we have demonstrated the feasibility of a SIPA-AD of point defects in a dislocation field. Furthermore, the SIPA-AD mechanism does not depend on a second-order contribution to the interaction energy which involves parameters difficult to evaluate such as the change of elastic constants due to point defects. In contrast, our proposed mechanism includes a lattice effect that seems not to depend on the detailed numerical values for the defect dipole tensor (as can be inferred from the results obtained using the three sets of dipole tensors reported by Schober[13]) but on the defect lattice symmetry in the equilibrium and the saddle-point configuration.

ACKNOWLEDGMENTS

This work was supported in part by the Comisión de Investigaciones Científicas de la Provincia de Buenos Aires (CIC), Argentina. We also acknowledge partial support from the Proyecto Multinacional de Tecnología de Materiales OAS-CNEA.

---

*Present address: Departamento de Física—Facultad de Ciencias Exactas, Universidad Nacional de Rosario, Pellegrini 250 (2000) Rosario, Argentina.

[1]F. S. Ham, J. Appl. Phys. 30, 915 (1959).
[2]L. G. Margvelashvili and Z. K. Saralidze, Fiz. Tverd. Tela (Leningrad) 15, 2665 (1973) [Sov. Phys.—Solid State 15, 1774 (1974)].
[3]W. G. Wolfer and M. Ashkin, J. Appl. Phys. 47, 791 (1976).
[4]H. Rauch and D. Simon, Phys. Status Solidi A 46, 499 (1978).
[5]L. A. Girifalco and D. O. Welch, *Point Defects and Diffusion in Strained Metals* (Gordon and Breach, New York, 1967).
[6]H. Kronmüller, W. Frank, and W. Hornung, Phys. Status Solidi B 46, 165 (1971).
[7]E. J. Savino, Philos. Mag. 36, 323 (1977).
[8]P. H. Dederichs and K. Schroeder, Phys. Rev. B 17, 2524 (1978).
[9]A. D. Brailsford, R. Bullough, and M. R. Hayns, J. Nucl. Mater. 60, 246 (1976).
[10]A. H. Cottrell and B. A. Bilby, Proc. Phys. Soc. London Sect. A 62, 49 (1949).
[11]R. Bullough and J. R. Willis, Philos. Mag. 31, 855 (1975).
[12]The factor $\frac{1}{2}$ in Eq. (1) originates from averaging the net flux of defects arriving and leaving at a given site, and it has been omitted by Kronmüller *et al.* (Ref. 6) and Savino (Ref. 7) in their earlier expressions.
[13]H. R. Schober, J. Phys. F 7, 1127 (1977).
[14]C. N. Tomé and E. J. Savino, Mater. Sci. Eng. 24, 109 (1976).
[15]F. R. N. Nabarro, *Theory of Crystal Dislocations* (Clarendon, Oxford, 1967).
[16]A. D. Brailsford and R. Bullough, Philos. Trans. R. Soc. London 302, 87 (1981).
[17]M. A. Burke and W. D. Nix, Philos. Mag. A 37, 479 (1978).
[18]E. J. Savino and C. N. Tomé, J. Nucl. Mater. (in press).
[19]R. Bullough and M. R. Hayns, J. Nucl. Mater. 57, 348 (1975).